Japanese Dental Science Review 61 (2025) 41–54

Contents lists available at ScienceDirect

Japanese Dental Science Review

journal homepage: www.elsevier.com/locate/jdsr

Micro- and nano-scale adhesion of oral bacteria to biomaterials using atomic force microscopy: A systematic review☆

Antonia Olivares [a], Valentina Barraza [a], Sebastian Aguayo [a,b,*]

[a] School of Dentistry, Faculty of Medicine, Pontificia Universidad Católica de Chile, Santiago, Chile
[b] Institute for Biological and Medical Engineering, Schools of Engineering, Medicine and Biological Sciences, Pontificia Universidad Católica de Chile, Chile

ARTICLE INFO

Keywords:
Atomic force microscopy
Single cell force spectroscopy
Oral bacteria
Adhesion
Systematic review
Bacterial adhesion

ABSTRACT

To evaluate the available evidence regarding in-vitro studies carried out with atomic force microscopy (AFM) to study the adhesion of oral bacteria under the research question: *"Which adhesion parameters have been reported for oral bacteria attachment to surfaces following AFM experiments?"*

This review was carried out following PRISMA guidelines. The Pubmed, Web of Science and Scopus databases were accessed and original articles reporting in-vitro findings on AFM-based oral bacteria adhesion experiments were included. Study selection and data extraction was performed by two independent researchers. Of the initial 249 screened articles, 24 were included in the final analysis.

Overall, the adhesion of oral bacteria to 12 different biomaterial surface types has been explored with AFM including soft materials, dental materials, and other materials. *S. mutans* was the most frequently studied bacterial species in its early attachment to biomaterials. Regarding AFM-based adhesion parameters, the maximum adhesion force, adhesion energy, rupture and contour lengths, and number of rupture events between oral bacteria and substrates have been quantified and reported.

Initial oral bacterial attachment to biomaterials is modulated by a range of cell, environmental, and surface-derived properties. Further research is needed to transfer this knowledge into the clinical setting.

1. Introduction

Despite current progress in diagnostics and treatment, dental caries and periodontal disease are still some of the most prevalent diseases worldwide, with an overall prevalence of oral diseases of around 3,47 billion cases [1,2]. These pathologies are promoted by complex microbial biofilms on the surface of the tooth [3]. More specifically, the dysbiosis of resident biofilms by the overgrowth of certain pathological species – such as *Streptococcus mutans* in dental caries and *Porphyromonas gingivalis* in periodontal disease – increases the local biofilm virulence and leads to tissue destruction [4]. Biofilm formation is a complex process that is initiated by the attachment of bacteria to surfaces [5]; therefore, the characterization of bacterial adhesion to tissues and biomaterials is crucial in finding novel ways to modulate or prevent disease in the oral cavity.

The adhesion of oral bacteria to biotic and abiotic surfaces follows a well-described process. In the initial stages, bacteria present in saliva approach the substrate due to salivary flow and interact with the surface through reversible Van der Waals and electrostatic forces [6]. These interactions usually occur at a bacterium-surface distance of >50 nm. If this physicochemical adhesion stage is favorable, the bacterium can come into close contact (<50 nm) with the surface and allow bacterial adhesins to generate irreversible attachment and promote bacterial division and extracellular matrix deposition [7]. Overall, adhesive forces between bacteria and surfaces depend on substrate characteristics, bacterial strain, and the surrounding environmental conditions [8]. Consequently, efforts are being placed to elucidate the factors determining bacterial adhesion and biofilm formation regarding cariogenic and periodontal biofilm formation.

As a result, over the years many techniques have been developed and optimized to study the behavior of bacterial adhesion. Among the most employed are microbiology-based assays (i.e., colony-forming units) and microscopy examination with electron and fluorescence microscopy. However, these techniques have several limitations including difficulties in differentiating adherent vs non-adherent bacteria, limited sensitivity, growth condition variability, and sample destruction during

☆ Scientific field of dental science: biomaterials research, oral microbiology.

* Correspondence to: Avda. Vicuña Mackenna 4860, Santiago de Chile, Macul, Chile
E-mail address: sebastian.aguayo@uc.cl (S. Aguayo).

https://doi.org/10.1016/j.jdsr.2025.03.002
Received 14 June 2024; Received in revised form 1 February 2025; Accepted 3 March 2025
Available online 17 March 2025

preparation and analysis [9]. Therefore, the development of advanced, non-invasive microscopy techniques such as atomic force microscopy (AFM) has revolutionized the field of bacterial adhesion studies [10]. AFM allows the simultaneous characterization of topographic and mechanical characteristics of samples in real-time, under near-physiological conditions [11]. Within the field of dentistry, its use has become relevant to study bacterial attachment to biomaterials, cells, tissues, and other bacteria of interest. The most common AFM techniques include bacterial force spectroscopy, a technique in which single bacteria are immobilized non-destructively and kept alive to probe their adhesive properties in real-time against substrates of interest [12,13] (Fig. 1). Bacteria can also be attached directly to the surface to study how surface or environmental factors modify the adhesive behavior of cells (Fig. 1). In both of these cases, AFM allows for the exploration of bacterial adhesion with microscale and nanoscale sensitivities. Thus, experimental data on adhesion force, adhesion work, and rupture lengths can be obtained for single cells all the way down to subcellular structures such as bacterial fimbriae, adhesins, and capsule [14].

However, despite the increasing use of AFM and bacterial force spectroscopy for exploring the mechanobiology of oral bacterial attachment, there are no reports that systematically summarize the available scientific evidence regarding the use of these approaches in dental research. Therefore, the objective of this systematic review is to evaluate the available evidence regarding studies carried out in vitro with AFM to study the adhesion of oral bacteria under the research question "which adhesion parameters have been reported for oral bacteria attachment to surfaces following AFM experiments?"

2. Materials and methods

2.1. Databases and search strategy

This systematic review followed the guidelines of the Preferred Reporting Items for Systematic Reviews and Meta-Analyses (PRISMA), and the search protocol was registered on the Open Science Foundation (OSF) platform. To facilitate the systematic literature search, the research question was formulated using the PICO strategy (Population: Oral bacteria; Intervention: AFM-based adhesion experiments; Comparison: none; Outcome: any reported adhesion parameters). The PubMed, Web of Science, and SCOPUS databases were last accessed in October 2023 to search for articles using specifically designed search strategies for each database (Supplementary Table 1). Original articles reporting *in-vitro* findings on AFM-based oral bacterial adhesion experiments and written in English were included. Exclusion criteria encompassed articles that used AFM solely for surface analysis and did not report on adhesion parameters, studies that employed patient-derived tissues or saliva, review and perspective articles, and full-text articles that were not retrievable for analysis.

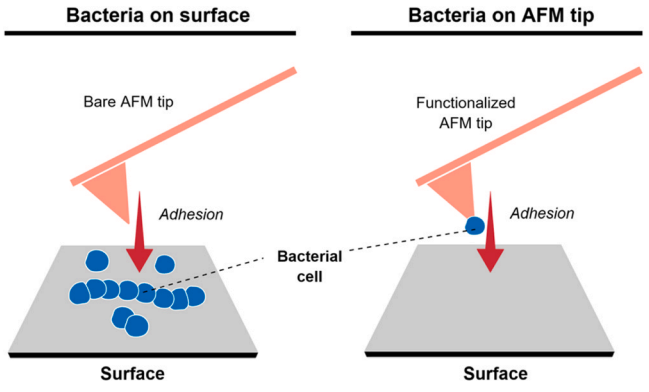

Fig. 1. Schematic representation of main atomic force microscopy (AFM) experimental setups to study the adhesion of oral bacteria to surfaces. Bacterial cells can be non-destructively immobilized either to a surface or to the tip of functionalized AFM probes to probe bacterial adhesion in real-time.

2.2. Study selection and data extraction

Study selection and data extraction was performed independently by two researchers (AO and VB). In cases of disagreement between the two researchers, the third researcher (SA) resolved the differences. From the initial search, 249 article abstracts were identified and screened, after which duplicated records (106 articles) as well as papers not related to the research question (91 articles) were removed (Fig. 2). Consequently, 52 articles were included for complete assessment. The information extracted from each article included the title, authors, DOI, journal name, year of publication, main objective, type of oral bacteria, type of surface, AFM adhesion outcomes, and main study conclusions. All these parameters were tabulated and summarized using a custom predesigned Excel spreadsheet.

Following the in-depth analysis of these 52 articles, a further 28 were excluded for 10 reasons pertaining to the previously determined inclusion and exclusion criteria. These reasons included experiments using saliva, experiments using non-oral bacteria, use of patient-derived cells or tissues, use of AFM for surface roughness and topography instead of bacterial adhesion, and use of bacterial derivates or biofilms instead of cells, amongst others (Fig. 2). Therefore, a final number of 24 articles were included for full assessment and are presented in this review.

3. Results

Overall, 12 different surfaces were reported as substrates for bacterial AFM adhesion experiments involving oral bacteria in the literature. These included soft materials (collagen, laminin, and fibronectin), restorative dental materials (clinically relevant biomaterials such as titanium and resins), and other materials (e.g., glass, polystyrene) (Table 1). Other materials such as glass, polystyrene, or bare AFM tips for experiments were also used as they allowed for the study of general substrate factors influencing adhesion such as hydrophobicity, attachment time, topography, and environmental conditions that are transferrable to oral biomaterials [15–18]. On the other hand, dental and soft materials were mostly selected to explore the adhesive behavior of relevant oral microorganisms in conditions that closely resemble the in-vivo situation, and in some cases, associated to physiological or pathological conditions such as bacterial tissue invasion or peri-implantitis [19–22]. Regarding the bacterial strains, *S. mutans* was the most studied microorganism and reports explore its adhesion to relevant biological and biomaterial surfaces such as collagen, fibronectin, laminin, glass ionomer, composites, zirconia, and hydroxyapatite (Table 1). To a lesser extent, the real-time adhesion of other relevant early and late colonizing oral microbes such as *Strepcococcus sanguinis*, *Streptococcus oralis*, and *Porphyromonas gingivalis* have also been studied with AFM-derived experiments (Table 1).

From an experimental point of view, the published protocols either involved functionalizing AFM probes with bacteria to examine their adhesion against a substrate of interest, or immobilizing living bacteria to a substrate to be probed with a bare or coated AFM tip (Fig. 1). From these experiments, the most reported AFM-based adhesion parameter was the maximum adhesion force between the bacterium and the substrate (Table 1). For oral bacteria, the reported maximum adhesion forces ranged from high pN to low nN values. Also, other relevant values such as the adhesion energy (also known as work of adhesion), minor unbinding forces, rupture or detachment length, total number of unbinding events, and contour lengths are shown [18,19,23,24]. Furthermore, all the studies that explored the role of contact time on adhesion concluded that the longer times lead to higher attachment forces between bacteria and the surface. Besides contact time, experimental variables such as type of buffer, contact force, and probing velocity are

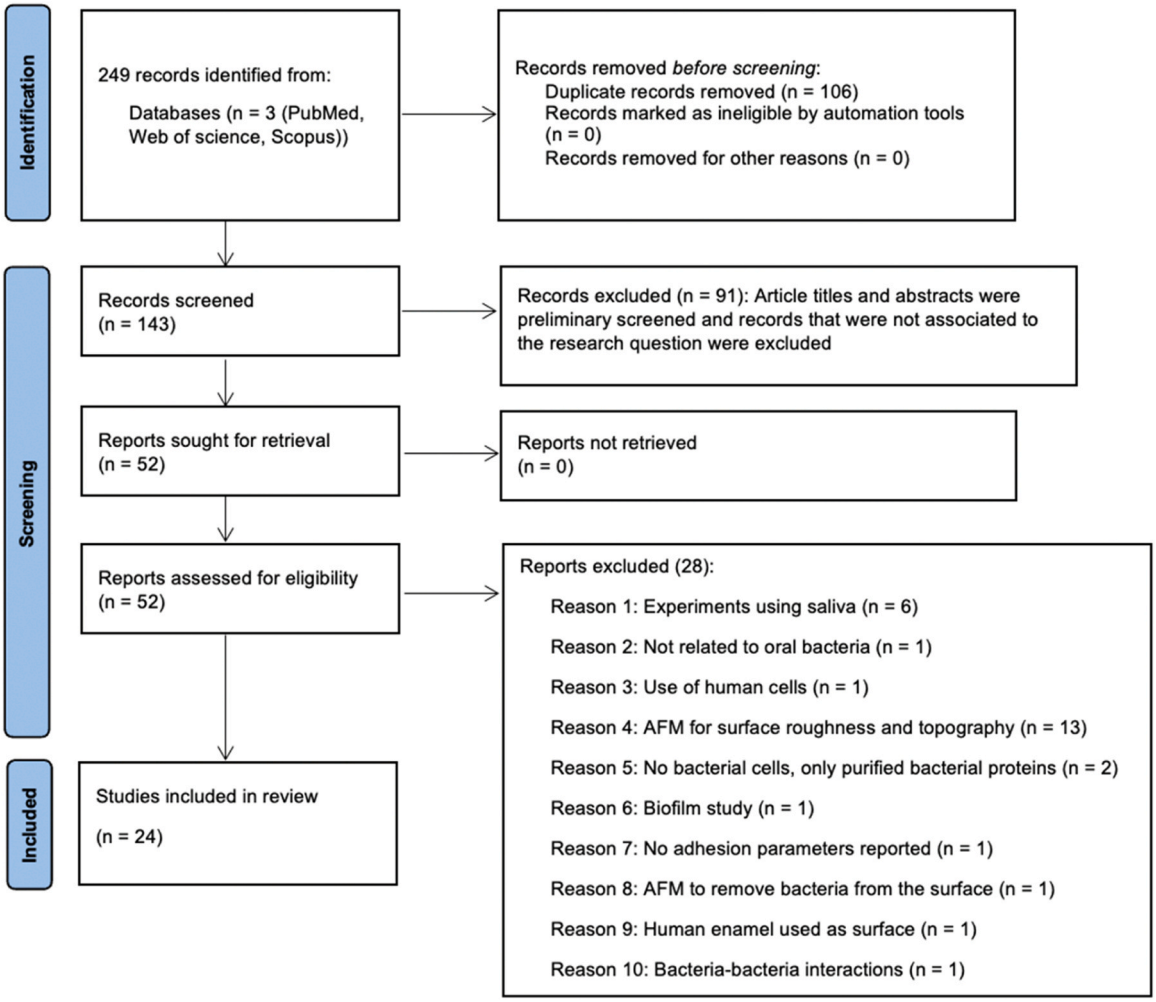

Fig. 2. PRISMA flowchart summarizing the article identification and screening process.

also reported and mostly showed an impact on adhesion results (Table 1).

Furthermore, significant adhesion differences were observed upon variations of the surface composition and the type of microbial strain used. For example, Schuh et al. and Leiva-Sabadini et al. found that glycation increases the adhesion of *S. mutans* but not *S. sanguinis* to type-I collagen surfaces [19,20]. González-Benito et al. showed that the incorporation of TiO2 into dental resins increased the adhesion forces and rupture length related to *S. mutans* attachment [23]. The opposite effect was observed by Dhall et al. when barium titanate was added to composites, as it reduced the attachment force of the bacteria [25]. Surface roughness was also found to promote *S. mutans* adhesion to zirconia [26]. Regarding bacterial cell differences, Wang et al. demonstrated that the deletion of the *gtfB* and *gtfC* genes, associated to glycosyltransferase (Gtfs) production, led to a reduction in the adhesion of *S. mutans* to glass ionomer and dental composite biomaterials [27]. Deletion of other relevant genes, such as *wapA*, *spaP*, and *luxS* were also found to alter the adhesion of *S. mutans* to silicon nitride, laminin, and glass [16,28,29]. Finally, it is also relevant to mention that fluor pretreatment of hydroxyapatite surfaces reduced the early adhesion of *S. carnosus, S. oralis,* and *S. mutans* when explored with AFM [30]. Similarly, the use of arginine was found to inhibit the early adhesion of *S. mutans* as well as the longer rupture lengths observed between the bacterial cell and surface [15]. Further information regarding detailed AFM adhesion results from these studies can be found summarized in Table 1.

4. Discussion

From the available results, it can be derived that there are many crucial biological parameters that influence oral bacterial adhesion onto substrates (Table 1). Among these, a higher contact time (also known as dwelling time) between the bacteria and surface leads to increased adhesion forces when probed with AFM. This can be explained by the process of bond strengthening, in which the bacteria can rearrange their membrane or cell wall components over time to optimize surface attachment that has also been observed in AFM experiments involving non-oral microorganisms [31,32]. This property can be clinically relevant, for example in patients that have a diminished crevicular fluid or salivary flow as this is a fundamental protective process that can remove bacteria from the surface [33]. Furthermore, one of the most important molecules mediating early bacterial attachment are adhesins, a family of surface receptors with the ability to sense the surface and adhere via a combination of physico-chemical and biological interactions [34,35]. Some relevant bacterial adhesins associated to oral biomaterial and tissue colonization include collagen-binding proteins such as SpaP, WapA, Gtfs, and the surface adhesion protein FimA [36,37]. Thus, the use of mutant strains defective in an adhesin (or another molecule) of interest is a frequently used method to understand the mechanisms behind bacterial adhesion. In all these cases, the deletion of an adhesin or Gtfs of interest leads to a reduction in the measured adhesion forces when explored with AFM [16,27–29,38].

Despite being a purely in-vitro method, bacterial adhesion experiments with AFM can provide important knowledge regarding clinical

Table 1
Summary of included studies on oral bacterial adhesion with atomic force microscopy (AFM).

1) Soft materials:
• Collagen:

Authors	Year	Bacteria	Probe type and spring constant	Measurement conditions	Surface Type	Surface roughness	AFM adhesion outcomes*	Main findings
Leiva-Sabadini, C. et al.	**2023**	***S. mutans* UA159** ***S. sanguinis* SK36**	**BL-TR400PB iDrive cantilevers (k ~0.09 N/m)**	**Liquid, PBS buffer**	**Type-I collagen gels (non-glycated and glycated with methylglyoxal, MGO)**	**Not specified**	**Median adhesion work (aJ):** ***S. mutans*: control (19.3) v/s glycated (34.7)** ***S. sanguinis*: control (48.8) v/s glycated (35.55).** **Mean single-unbinding forces (nN) *S. mutans*: control (0.07 ± 0.04) v/s glycated (0.3 ± 0.33)** ***S. sanguinis*: control (0.14 ± 0.1) v/s glycated (0.12 ± 0.07).** **Rupture and contour lengths:** **Median ~200 nm; most ruptures < 400 nm.** **Minor unbinding peaks (nN):** ***S. mutans*: control (265); glycated (400).** ***S. sanguinis*: control (795); glycated (446)**	**Increase in adhesion work and single-unbinding forces for *S. mutans* following collagen glycation, with the opposite observed for *S. sanguinis*.** **With respect to rupture and contour lengths, no changes were observed between native and glycated collagen for both strains.**
Schuh, C.M.A.P. et al.	**2020**	***S. mutans* UA159** ***S. sanguinis* SK36**	**BL-TR400PB iDrive cantilevers (k ~0.09 N/m)**	**Liquid, PBS buffer**	**Type-I collagen gels (non-glycated and glycated with glucose and MGO)**	**92.3 ± 6.7 nm for control surfaces; 100.4 ± 7.1 nm for glucose-crosslinked collagen; and 87.6 ± 5.2 nm for methylglyoxal (MGO)-crosslinked collagen**	**Maximum adhesion force (nN):** **At 0 and 5 s dwelling times** ***S. mutans:* 0.14 (control); 0.21 (glucose); 0.23 (MGO).** ***S. sanguinis:* 0.44 (control); 0.26 (glucose); 0.23 (MGO).**	**A significant increase in adhesion was observed with *S. mutans* when probed against collagen gels modified with glucose or MGO. On the contrary, *S. sanguinis* presented a significant decrease in its adhesion following collagen glycation. In all cases, increased time led to increased adhesion.**
•Fibronectin:								
Busscher, H.J. et al.	**2008**	***S. mutans* L11** ***S. intermedius* NCTC 11324**	**NP with a nominal tip radius of 20 nm (k~0.06 N/m)**	**Liquid, PBS buffer**	**Fibronectin-Coated AFM tips in high and low ionic strength PBS**	**Not specified**	**Repulsive force at contact (nN):** ***S. mutans:*** **Median: PBS (10.8) v/s PBS/10 (5.5)** **Mode: PBS (10.9) v/s PBS/10 (2.3)** **Range: PBS (24.2) v/s PBS/10 (18.2)** ***S. intermedius:*** **Median: PBS (8.2) v/s PBS/10 (7.8)** **Mode: PBS (7.2) v/s PBS/10 (9.6)** **Range: PBS (15) v/s PBS/10 (10.7)**	***S. mutans* showed higher values of repulsive force at contact when compared to *S. intermedius* in high ionic strength PBS. On the contrary, *S. intermedius* showed increased values when in low ionic strength PBS.** **The repulsive force median range for *S. intermedius* between high and low ionic strength PBS is smaller when compared to *S. mutans*.** **In general, *S. mutans* shows higher values of adhesion**

(*continued on next page*)

Table 1 (*continued*)

							Repulsive force range (nm): ***S. mutans:*** **Median: PBS (38) v/s PBS/10 (19)** **Mode: PBS (6) v/s PBS/10 (15)** **Range: PBS (225) v/s PBS/10 (38)** ***S. intermedius:*** **Median: PBS (35) v/s PBS/10 (29)** **Mode: PBS (22) v/s PBS/10 (33)** **Range: PBS (390) v/s PBS/10 (133)** **Adhesion force (nN):** ***S. mutans:*** **Median: PBS (0.2) v/s PBS/10 (0.2)** **Mode: PBS (0.1) v/s PBS/10 (0.2)** **Range: PBS (4.7) v/s PBS/10 (4.3)** ***S. intermedius:*** **Median: PBS (0.1) v/s PBS/10 (0.0)** **Mode: PBS (0.0) v/s PBS/10 (0.0)** **Range: PBS (3.2) v/s PBS/10 (0.9)**	**force when compared to *S. intermedius*, for both high and low ionic strength PBS.**
•Laminin:								
Busscher, H.J. et al.	**2007**	***S. mutans* LT11 + antigen I/II isogenic mutant (IB03987)**	**NP with a nominal tip radius of 20 nm (k∼0.06 N/m)**	**Liquid; 2 mM potassium phosphate, 50 mM potassium chloride, 1 mM calcium chloride buffer**	**Laminin films**	**Not specified**	**Repulsive force at contact (nN):** ***S. mutans* LT11:** **Median: pH 5.8 (6.3) v/s pH 6.8 (5.7)** **Mode: pH 5.8 (6.6) v/s pH 6.8 (3.7)** **Range: pH 5.8 (9.0) v/s pH 6.8 (9.4)** ***S. mutans* IB03987:** **Median: pH 5.8 (8.9) v/s pH 6.8 (8.3)** **Mode: pH 5.8 (9.4) v/s pH 6.8 (8.3)** **Range: pH 5.8 (12.7) v/s pH 6.8 (11.6)** **Repulsive force range (nm):** ***S. mutans* LT11:** **Median: pH 5.8 (28) v/s pH 6.8 (28)** **Mode: pH 5.8 (41) v/s pH 6.8 (32)** **Range: pH 5.8 (120) v/s pH 6.8 (83)** ***S. mutans* IB03987:**	**Significant differences between repulsive forces at contact between both *S. mutans* strains. Furthermore, the pH did not have a significant effect on adhesion.** **Overall, adhesion forces were greater for *S. mutans* LT11, acquiring a significant difference with *S. mutans* IB03987 at pH 6.8.**

(*continued on next page*)

Table 1 (*continued*)

							Median: pH 5.8 (40) v/s pH 6.8 (29) Mode: pH 5.8 (40) v/s pH 6.8 (31) Range: pH 5.8 (205) v/s pH 6.8 (104) Adhesion force (nN): *S. mutans* LT11: Median: pH 5.8 (0.0) v/s pH 6.8 (−0.1) Mode: pH 5.8 (0.0) v/s pH 6.8 (−0.1) Range: pH 5.8 (−5.0) v/s pH 6.8 (−4.9) *S. mutans* IB03987: Median: pH 5.8 (0.0) v/s pH 6.8 (0.0) Mode: pH 5.8 (0.0) v/s pH 6.8 (0.0) Range: pH 5.8 (−1.5) v/s pH 6.8 (−2.1)	
2) Restorative dental materials: • Glass ionomer composite (GIC)								
Wang, R. et al.	2022	*S. mutans* UA159, gtfB and gtfC mutants (ΔgtfB and ΔgtfC)	Tipless AFM probe CSC37/ tipless/Cr-Au (k~0.3 N/m)	Liquid, PBS buffer	GIC (Fuji IX, GC Corp.)	20 ± 5 nm	Cell–surface adhesion forces of *S. mutans* on GIC (nN): Wild type: 1.48 ± 0.66 ΔgtfB: 0.97 ± 0.55 ΔgtfC: 0.73 ± 0.54	The adhesion force of S. mutans UA159 (wild type) to GIC was significantly higher than for both mutant strains. Furthermore, results between mutants appeared to be alike.
•Composites:								
Wang, R. et al.	2022	*S. mutans* UA159, gtfB and gtfC mutants (ΔgtfB and ΔgtfC)	Tipless AFM probe CSC37/ tipless/Cr-Au (k~0.3 N/m)	Liquid, PBS buffer	Composite resin (Z250; 3 M ESPE Dental Products)	20 ± 5 nm	Cell–surface adhesion forces of *S. mutans* on composite resin (nN): Wild type: 1.01 ± 0.55 ΔgtfB: 0.68 ± 0.43 ΔgtfC: 0.61 ± 0.32	The adhesion force of S. mutans UA159 (wild type) to composite resin was significantly higher than for both mutant strains. Furthermore, results between mutants appeared to be alike.
González-Benito, J. et al.	2017	*S. mutans* ATCC25175	Tipless NP−010 cantilever (k~0.06 N/m)	Liquid, PBS buffer	PVDF/TiO_2 nanocomposites with different TiO_2 composition (0 %, 1 %, 2 %, 5 % and 10 % by weight)	PVDF−0 %: 1.90 ± 0.20 (Rq (μm)), 1.34 ± 0.22 (Ra (μm)) PVDF−1 %: 0.51 ± 0.30 (Rq (μm)), 0.38 ± 0.25 (Ra (μm)) PVDF−2 %: 1.43 ± 0.42 (Rq (μm)), 0.89 ± 0.31 (Ra (μm)) PVDF−5 %: 7.00 ± 0.93 (Rq (μm)), 4.28 ± 0.70 (Ra (μm)) PVDF−10 %: 0.37 ± 0.22 (Rq (μm)), 0.26 ± 0.18 (Ra (μm)) PVDF−0 % (bottom): 0.09 ± 0.01 (Rq (μm)), 0.05 ± 0.01 (Ra (μm)) PVDF−5 % (bottom):	Mean adhesion force (nN): PVDF: 0.404 ± 0.235 PVDF/TiO_2 5 %: 1.277 ± 0.510 Mean rupture length (nm): PVDF: 67.7 ± 27.2 PVDF/TiO_2 5 %: 82.5 ± 21.8	Modifying PVDF with 5 % TiO_2 led to higher *S. mutans* adhesion forces when compared to pure PVDF.

(*continued on next page*)

Table 1 (*continued*)

Dhall, A. et al.	**2021**	***S. mutans* UA159**	**Tipless PNP-TR-TL—50 cantilever**	**Liquid, PBS buffer**	**Nanocomposite disks with and without Barium Titanate (BTO)**	**0.23 ± 0.04 (Rq (μm)), 0.17 ± 0.03 (Ra (μm)) 30 wt% BTO: 80 nm; control 20 nm (Sa)**	**Binding force distribution:** ***S. mutans* − control disks: ~50 % of the adhesion force values between 1 and 1.6 nN. Maximum force: 2.51 nN.** ***S. mutans* − BTO-nanocomposite disks: ~70 % of the adhesion force values between 0.4 and 1 nN. Maximum force: 1.09 nN.**	***S. mutans* showed lower adhesion forces when interacting with nanocomposite disks modified with BTO in comparison to control disks.**
• Zirconia:								
Yu, P. et al.	**2016**	***S. mutans* UA159**	**CSC37/Tipless cantilevers (k~0.3 N/m)**	**Liquid, PBS buffer**	**Zirconia disks sorted in 3 groups with varying surface roughness: coarse, medium, and fine**	**Surface roughness (Ra): Coarse: 23.94 ± 2.52 nm Medium: 17.00 ± 3.81 nm Fine: 11.89 ± 1.68 nm**	**Mean adhesion force (nN): Coarse: ~ 6 Medium: ~ 4 Fine: ~ 2**	**The adhesion of S. mutans increased at higher surface roughness, with significant results being observed among the three groups.**
• Titanium:								
Aguayo, S. et al.	**2016**	***S. sanguinis* ATCC 10556**	**NP-S10 probes (k = 0.3 N/m)**	**Liquid, TRIS buffer and 2 mg/ml chlorhexidine solution in TRIS buffer**	**Titanium surfaces**	Titanium (Ra): 0.61 ± 0.01 μm conventional profilometry; 0.17 ± 0.02 μm AFM profilometry	Adhesion force (nN): 0 s contact time: 0.32 ± 0.00 1 s contact time: 1.07 ± 0.06 60 s contact time: 4.85 ± 0.56 Adhesion work (aJ): 0 s contact time: 19.28 ± 2.38 1 s contact time: 104.60 ± 7.02 60 s contact time: 1317.26 ± 197.69	**Increased contact times between *S. sanguinis* and Ti yield higher adhesion forces, predominantly through short-range forces. Chlorhexidine treatment of the surface increased adhesion forces.**
Doll-Nikutta, K. et al.	**2022**	***S. oralis* ATCC 9811** ***A. naeslundii* DSM 43013** ***V. dispar* DSM 20735** ***P. gingivalis* DSM 20709** ***A. actinomycetemcomitans* JP2 strain (HK1651, CCUG 56173)**	**FluidFM Nanopipette (k = 0.6 N/m)**	**Liquid, PBS and RTF (anaerobe-reduced transport fluid) buffers**	**Titanium surfaces**	**Arithmetic mean roughness (Ra) = 0.3 ± 0.05 μm Average surface roughness (Rz) = 2.6 ± 0.1 μm Maximum roughness depth (Rmax) = 3.3 ± 0.2 μm**	**Maximum adhesion force (nN):** ***S. oralis:*** **PBS (2.19 ± 1.34) v/s RTF (0.47 ± 0.51)** ***A. naeslundii:*** **PBS (0.56 ± 0.31) v/s RTF (0.40 ± 0.28)** ***V. dispar:*** **PBS (0.28 ± 0.20) v/s RTF (0.18 ± 0.12)** ***P. gingivalis:*** **PBS (0.45 ± 0.33) v/s RTF (0.51 ± 0.44)** ***A. ac* rough colonies:** **PBS (0.37 ± 0.23) v/s RTF (0.24 ± 0.30)** ***A. ac* smooth colonies:** **PBS (0.37 ± 0.23) v/s RTF (0.28 ± 0.13)**	**Adhesion results tend to be buffer specific, where overall PBS shows higher values compared to RTF. Bacterial adhesion in both buffers were significantly different for each species except for *P. gingivalis*. Maximum adhesion forces for *A. ac* from rough and smooth colonies were only different in RTF buffer.**

(*continued on next page*)

Table 1 (*continued*)

Doll, K. et al.	**2019**	***S. oralis* ATCC−9811**	**FluidFM Nanopipette (k = 0.6 N/m)**	**Liquid, PBS buffer**	**Titanium with and without antifouling pre-treatment (SLIPS)**	**Not specified**	**Max adhesion force (nN):** **Adhesion time 0 s:** **Titanium (0.82 ± 0.50)** **v/s SLIPS (0.84 ± 0.56)** **Adhesion time 10 s:** **Titanium (1.44 ± 1.00)** **v/s SLIPS (1.24 ± 0.63)** **Adhesion time 30 s:** **Titanium (3.67 ± 2.16)** **v/s SLIPS (2.70 ± 1.34)**	**Increase in maximum adhesion force as contact time increases for both surfaces was found. Only significant differences were observed at 30 second adhesion times.**
Imran Rahim, M. et al.	**2021**	***S. oralis* ATCC 9811** ***P. gingivalis* DSM 20709**	**FluidFM Nanopipette (k = 0.6 N/m)**	**Liquid, PBS buffer**	**Titanium with and without *S. oralis* pre-coating**	**Not specified**	**Maximum adhesion force (nN):** ***S. oralis:*** **Uncoated titanium: ~ 3–5** **Coated titanium: ~ 0.3–1** ***P. gingivalis:*** **Uncoated titanium: ~ 2–3** **Coated titanium: ~ 0.2–0.5**	**For both bacterial species, maximum adhesion forces were increased on uncoated titanium compared to *S. oralis* coated titanium**
•Hydroxyapatite:								
Loskill, P. et al.	**2013**	**Clinical isolates *S. mutans* and *S. oralis*** ***S. carnosus* TM 300**	**Tipless MLCT−0 and PNP-TR_TL cantilevers**	**Liquid, PBS buffer**	**Hydroxyapatite surfaces with and without fluor**	**RMS: 5 nm**	**Relative adhesion force (nN):** ***S. carnosus:*** **Untreated surface: ~ 1.0** **Treated surface: ~ 0.6** ***S. mutans:*** **Untreated surface: ~ 1.0** **Treated surface: ~ 0.5** ***S. oralis:*** **Untreated surface: ~ 1.0** **Treated surface: ~ 0.5**	**Fluoride treatment reduced adhesion force for all three bacteria when compared to untreated hydroxyapatite surfaces.**
1) Other materials:								
•Glass:								
Das, T. et al.	**2011**	***S. mutans* L11 with and without eDNA**	**Tipless DNP−0 cantilevers**	**Liquid, high and low ionic strength PBS buffer**	**Glass – hydrophobic and hydrophilic**	**Not specified**	**Maximum adhesion force (nN):** **Increased with dwelling times from 0 to 120 s** **Hydrophilic surfaces: < ~10** **Hydrophobic surfaces: < ~35** **Rupture distance (nm):** **Hydrophilic surfaces: < ~500** **Hydrophobic surfaces: < ~1000 in 150 mM PBS; < ~200 in 15 mM PBS.** **Number of adhesion peaks (n):** **Hydrophilic surfaces: ~2–6** **Hydrophobic surfaces: < ~2**	**Bacterial adhesion increased at higher cell-surface contact times. eDNA promoted streptococcal attachment, particularly on hydrophobic surfaces. Also, ionic strength increased adhesion forces.**
Preedy, E. et al.	**2014**	***S. epidermidis* RP62 and ATCC 12228**	**Not specified**	**Liquid, PBS buffer**	**Borosilicate glass, with and without bovine serum albumin (BSA)**	**Roughness scale (nm) ranges:** **Micro:**	**Median adhesion forces (nN):** ***S. epidermidis* RP62:**	**Adhesion forces between clean glass and *S. mutans* were the lowest compared to**

(*continued on next page*)

Table 1 (*continued*)

		S. aureus **ATCC 25923** ***S. mutans*** **NCTC 10449**			**coating and different micro and nanoscale roughness** **5 groups (A: control; B-C-D-E: increasing roughness)**	**0.250–94.40 nm** **Nano:** **0.259–62.15 nm** **Micro after BSA coating: 1.54–145.88 nm** **Nano after BSA coating: 1.35–4.25 nm**	**Clean glass samples: Group A (4.25), B (4.2), C (11.5), D (17.5) and E (42)** **BSA-coated glass samples: Group A (2.75), B (3.25), C (4.0), D (2.5) and E (6.25)** ***S. epidermidis*** **ATCC 12228:** **Clean glass samples: Group A (2.0), B (7.6), C (6.0), D (4.6) and E (7.8)** **BSA-coated glass samples: Group A (1.5), B (2.75), C (6.0), D (2.75) and E (5.5)** ***S. aureus*** **ATCC 25923:** **Clean glass samples: Group A (5.75), B (9.25), C (9.75), D (10.5) and E (9.0)** **BSA-coated glass samples: Group A (2.75), B (3.0), C (1.5), D (5.25) and E (1.25)** ***S, mutans*** **NCTC 10449:** **Clean glass samples: Group A (4.75), B (2.5), C (3.0), D (3.2) and E (3.75)** **BSA-coated glass samples: Group A (0.75), B (5.5), C (12), D (14) and E (24)**	**other species, independent of surface roughness.** ***S. epidermis*** **RP62 demonstrated the highest adhesion force on clean glass, increasing its value as the surface roughness increased. On the other hand,** ***S. mutans*** **showed the highest adhesion values on BSA-coated glass in comparison to other bacterial species, which increased with surface roughness.**
Sjollema, J. et al.	**2017**	***S. aureus*** **NCTC 8325–4** ***S. mutans*** **LT11 and IB 03987** ***S. salivarius*** **HB7 and HBC−12**	**Tipless NPO cantilevers (k: 0.04 N/m)**	**Liquid; 10 mM potassium phosphate buffer, pH 6.8**	**Glass (Menzel GmbH, Braunschweig, Germany)**	**Not specified**	**Adhesion force (nN):** ***S. aureus*** **NCTC8325–4: (1.4 ± 0.2)** ***S. mutans*****: LT11 (1.8 ± 0.2) v/s IB03987 (0.6 ± 0.2)** ***S. salivarius*****: HB7 (1.1 ± 0.1) v/s HBC−12 (1.0 ± 0.1)**	**Bacterial adhesion is modulated by reversibly binding tethers that detach and reattach to surfaces. Compared to previous studies, the adhesion force values for these studied strains are within a similar range (low nN) to previously studied bacteria.**
Wang, C. et al.	**2019**	***S. mutans*** **UA 159 + isogenic mutant form (Δ*luxS*)**	**Tipless NP-O10 cantilever (k: 0.03–0.12 N/m)**	**Liquid; 1 mM CaCl2, 2 mM potassium phosphate, 50 mM KCl buffer at pH 6.8**	**Glass (Thermo Scientific, Braunschweig, Germany)**	**Not specified**	**Initial adhesion force (nN):** **Wild type 0.7 ± 0.1** **Δ*luxS* 0.8 ± 0.5** **Stationary adhesion force (nN):** **Wild type 4.1 ± 1.3** **Δ*luxS* 3.3 ± 2.7**	***S. mutans*** **adhesion forces were associated to specific gene expression in the biofilm, such as** ***brpA*** **and** ***gbpB*****. Initial adhesion forces were all in the sub-nN range for the parent and the isogenic mutant strain. Overall, results support the notion that force sensitivity of bacterial attachment modulates their biofilm behavior.**

(*continued on next page*)

Table 1 (*continued*)

•Bare AFM tip (silicon nitrate):								
Vadillo-Rodríguez, V. et al.	2004[a]	*S. mitis* ATCC 9811, ATCC 33399, 244, 272, 357, 398, BMS, BA, T9	'V'-shaped silicon nitride cantilevers (k: 0·06 N/m)	Liquid, 0.1 M KCl solution	Bare AFM tip	Not specified	Mean adhesion force (nN): ATCC 9811: 0.5 ± 0.3 ATCC 33399: 1.4 ± 0.8 244: 1.8 ± 1.0 272: 1.0 ± 0.4 357: 0.7 ± 0.2 398: 1.5 ± 0.7 BMS: 1.1 ± 0.4 BA: 1.4 ± 0.3 T9: 2.2 ± 0.9	Values of mean adhesion forces for the different *S. mitis* strains varied between 0.5 and 2.2 nN, depending on the different strain types.
Vadillo-Rodríguez, V. et al.	2004[b]	*S. thermophilus* B isolate	'V'-shaped silicon nitride cantilevers (k: 0·06 N/m)	Liquid, 40 mM potassium phosphate solution at pH 2 and 7	Bare AFM tip	Not specified	Maximum adhesion force (nN): Time 10 s: pH 2 (~1) v/s pH 7 (~1.5) Time 50 s: pH 2 (~2.5) v/s pH 7 (~2) Time ~90s: pH 2 (~3.5) v/s pH 7 (~2.75) Time 130 s: pH 2 (~2.75) v/s pH 7 (~3.5) Time 170 s: pH 2 (~2.5) v/s pH 7 (~4) Time 200 s: pH 2 (~4) v/s pH 7 (~3.5)	Adhesion force for *S. thermophilus* increased over time at both studied pH.
Cross, S.E. et al.	2007	*S. mutans* UA 140 and Gtf mutants	OTR4 silicon nitride cantilevers (k: 0.02 N/m)	Liquid, BHI buffer	Bare AFM tip	Not specified	Mean rupture force (pN): Wild-type control, 6 h and 12 h sucrose-treated cells: 84.1 ± 156.0, 304.3 ± 281.9 and 375.6 ± 563.2, respectively UA140 gtfB: control cells 46.1 ± 80.6 v/s 12 h sucrose-treated 53.0 ± 148.3 UA140 gtfC: control cells 42.0 ± 28.5 v/s 12 h sucrose-treated 43.9 ± 68.8 UA140 gtfD: control cells 42.7 ± 22.4 v/s 12 h sucrose-treated 111.3 ± 128.2 UA140 gtfBC: control cells 35.1 ± 22.4 v/s 12 h sucrose-treated 53.2 ± 46.0 UA140 gtfBCD: control cells 36.3 ± 17.3 v/s 12 h sucrose-treated 37.4 ± 14.2	*S. mutans* cells adhere to surfaces mainly through glucans in the presence of sucrose. Also, the adhesion force increases in a time dependent manner.
Vadillo-Rodríguez, V. et al.	2003	*S. mitis* ATCC 9811, ATCC 33399, 244, 272, 357, 398, BMS, BA, T9	'V'-shaped silicon nitride	Liquid, deionized water or 0.1 M KCl solution	Bare AFM tip	Not specified	Average adhesion force in water (nN): ATCC9811 (1.3 ± 0.6);	Adhesion forces were higher in water than 0.1 M KCl for *S. mitis* ATCC9811, 357, and BA.

(*continued on next page*)

Table 1 (*continued*)

			cantilevers (k: 0·06 N/m)				ATCC33399 (1.3 ± 0.8); 244 (0.9 ± 0.4); 272 (1.3 ± 0.7); 357 (1.3 ± 0.3); 398 (1.8 ± 1.0); BMS (1.5 ± 0.8); BA (2.9 ± 1.2); T9 (1.4 ± 0.8) Average adhesion force in 0.1 M KCl (nN): ATCC9811 (0.5 ± 0.4); ATCC33399 (1.4 ± 0.9); 244 (1.8 ± 1.1); 272 (1.0 ± 0.5); 357 (0.7 ± 0.3); 398 (1.5 ± 0.7); BMS (1.1 ± 0.4); BA (1.4 ± 0.3); T9 (2.2 ± 1.0)	Adhesion forces were lower in water than 0.1 M KCl for *S. mitis* 244, 398, and BMS. *S. mitis* ATCC33399, 272, and T9 strains did not show adhesion differences.
Zhu, L. et al.	2006	*S. mutans* UA 140 and its *wapA* deficient mutant	Sharpened silicon nitride cantilevers (k: 0.02 N/m)	Liquid, BHI buffer	Bare AFM tip	Control bacteria mean surface roughness Wild-type: 7.20 ± 1.31 nm wapA mutant: 5.43 ± 0.74 nm Sucrose exposed mean surface roughness Wild-type: 9.76 ± 0.95 nm wapA mutant: 9.63 ± 0.93 nm	Mean rupture force (pN): *wapA* mutant: 43 ± 13 UA140 wild-type: 84 ± 156 Range of rupture events (pN): *wapA* mutant: ~20–80 UA140 wild-type: ~20–330	The cell surface of the wapA mutant was less adhesive than the wild type. Overall, wild-type bacteria showed considerably more frequent adhesion events than the mutant cell, suggesting that WapA plays a crucial role in aggregation and biofilm formation.
Sharma, S. et al.	2014	*S. mutans* UA 140, in presence or absence of arginine or glycine	Sharpened silicon nitride MLCT cantilevers (k: 0.01 N/m)	Liquid, PBS buffer	Bare AFM tip	Biofilm surface roughness was measured as Ra, Rq, and Rmax: Arginine: 52 nm, 42.8 nm and 297 nm, respectively. Arginine-free: 89.1 nm, 67.3 nm and 515 nm, respectively,	Mean adhesion force (nN): Control: 3.5 ± 0.6 Arginine: Biofilm grown under 0.5 mg ml^{-1}: 3.1 ± 2.4 Biofilm grown under 1 mg ml^{-1}: 1.4 ± 0.7 Biofilm grown under 5 mg ml^{-1}: 1.3 ± 0.6 Glycine: Biofilm grown under 1 mg ml^{-1}: 3.7 ± 1.4 Biofilm grown under 5 mg ml^{-1}: 3.8 ± 1.8 Mean rupture lengths (nm): Absence: 1400 ± 800 (peak 1); 6500 ± 100 (peak 2) Arginine: Biofilm grown under 0.5 mg ml^{-1}: 1500 ± 100 (peak 1); 5900 ± 100 (peak 2) Biofilm grown under 1 mg ml^{-1}: 1600 ± 100 (peak 1); 4800 ± 200 (peak 2) Biofilm grown under	Arginine concentrations of 1 mg ml^{-1} and above diminished the adhesion forces of *S. mutans*, clustering at less than 2 nN. Glycine did not show the same effect. Furthermore, the rupture length population associated to the larger peak showed a gradual and significant reduction upon treatment with arginine, suggesting a potential anti-biofilm effect for the molecule.

(*continued on next page*)

Table 1 (*continued*)

							5 mg ml^{-1}: 1500 ± 100 (peak 1); 4500 ± 200 (peak 2) Glycine: Biofilm grown under 1 mg ml^{-1}: 1900 ± 100 (peak 1); 5800 ± 200 (peak 2) Biofilm grown under 5 mg ml^{-1}: 1500 ± 500 (peak 1); 5700 ± 200 (peak 2)	
Liu, B.H. and Yu, L-C.	2017	*S. mutans* ATCC 25175	RTESPA silicon probes	Not specified	Bare AFM tip	Not specified	Mean adhesion force (nN): Initial attachment: ~150nN EPS regions: ~60 (20 min, initial adhesion) to ~85 (120 min).	Adhesion forces increase with biofilm maturation, suggesting EPS secretion over time, particularly in the region surrounding the live cells. Early attachment shows reduced adhesion force compared to mature biofilms.
•Polystyrene:								
Wang, C. et al.	2019	*S. mutans* UA 159 + isogenic mutant form (Δ*luxS)*	Tipless NP-O10 cantilevers (k: 0.03–0.12 N/m)	Liquid; 1 mM CaCl2, 2 mM potassium phosphate, 50 mM KCl buffer at pH 6.8	Tissue-grade polystrene (Greiner Bio-One GmbH)	Not specified	Initial adhesion force (nN): Wild type: 0.5 ± 0.4 Δ*luxS:* 0.2 ± 0.1 Stationary adhesion force (nN): Wild type: 4.1 ± 0.8 Δ*luxS:* 4.7 ± 2.6	Initial forces were all in the sub-nN range for both strains, and the final stationary forces were similar amongst the 2 studied bacteria. In both cases, the adhesion force increased with longer contact times (from 0 to 30 ss).
Wang, C. et al.	2019	*S. mutans* UA 159 + isogenic mutant form (Δ*luxS)*	Tipless NP-O10 cantilevers (k: 0.03–0.12 N/m)	Liquid; 1 mM CaCl2, 2 mM potassium phosphate, 50 mM KCl buffer at pH 6.8	Bacterial-grade polystyrene (Greiner Bio-One GmbH, Frickenhausen, Germany)	Not specified	Initial adhesion force (nN): Wild type: 0.8 ± 0.5 Δ*luxS:* 1.0 ± 0.6 Stationary adhesion force (nN): Wild type: 6.1 ± 2.4 Δ*luxS:* 8.4 ± 7.3	The *luxS* mutant showed an increased adhesion force to the surface compared to the wild-type parent strain.
•Silicon rubber:								
Wang, C. et al.	2019	*S. mutans* UA 159 + isogenic mutant form (Δ*luxS)*	Tipless NP-O10 cantilevers (k: 0.03–0.12 N/m)	Liquid; 1 mM CaCl2, 2 mM potassium phosphate, 50 mM KCl buffer at pH 6.8	Silicon rubber (ATOS Medical B.V., Zoetermeer, The Netherlands)	Not specified	Initial adhesion force (nN): Wild type 1.2 ± 0.4 Δ*luxS* 0.9 ± 0.6 Stationary adhesion force (nN): Wild type 19.2 ± 14.0 Δ*luxS* 20.2 ± 13.7	Bond maturation happened at a slower rate in the *S. mutans* parent strain. Compared to glass surfaces, the difference in adhesion to silicone rubber surfaces was significant within each strain.

k: cantilever spring constant

* : as adhesion forces are vectorial, in some studies they are reported as negative values. Thus, this table only reports the absolute values of adhesion.

parameters that govern oral bacterial adhesion to tissues. For example, it is interesting to observe that early oral colonizers demonstrate an increased affinity with a range of natural and artificial surfaces in the oral cavity [21,39]. This suggests that early oral colonizers – particularly oral streptococci – have evolved a plethora of mechanisms that allow them to interact with the host even in the absence of a salivary pellicle [40]. Furthermore, AFM assays involving oral bacterial adhesion to soft biomaterials usually yield lower experimental adhesion parameters compared to hard surfaces or materials. This is probably due to substrate compliance during surface-bacteria binding that allows for a reduced number of molecular interactions during the experiment [20]. Furthermore, other clinically extrapolatable variables that modulate bacterial attachment include surface roughness, surface glycation, presence of fluor, and presence of antifouling agents [19,26,30,41,42]. Nevertheless, further studies are needed to examine if the impact of these parameters on early bacterial adhesion also transfers to the biofilm maturation level, as well as to the promotion or inhibition of biofilm dysbiosis associated with oral diseases [4].

Among the most studied bacteria, the adhesion of *S. mutans* and particularly the UA 159 strain to surfaces is the most frequently used in-vitro model for AFM experimentation. One possible explanation for this is that its genome is fully sequenced and therefore allows for the association of adhesion experiments with other biological and molecular results [43,44]. Overall, *S. mutans* is one of the most studied microbes in association with dental caries and therefore its adhesion to biological and artificial surfaces has been explored in several published reports [45]. It is also implicated in remote tissue invasion and colonization that is particularly associated to its collagen binding properties [46–48]. On the other hand, the colonization of titanium substrates by early colonizers such as *S. sanguinis* and *S. oralis* has been explored in the context of dental implant biofilm formation, as well as adhesion by the pathogenic *P. gingivalis* that is strongly associated with biofilm dysbiosis and peri-implant tissue destruction [49]. Therefore, AFM-based experiments are highly relevant for understanding the role of bio-tribocorrosion on peri-implant physiopathology [50] and searching for novel surface configurations and molecules that can inhibit biofilm formation in this context.

From an experimental point of view, it remains important to comprehend the AFM adhesion parameters being reported in each paper. For example, the most used measurement is the maximum adhesion force that reflects the strongest interaction point between the bacterial cell and surface [51]. For oral bacteria, results consistently show maximum adhesion forces in the nN and pN range, similar to what is seen in AFM experiments involving other bacteria [52,53]. However, it is also possible to evaluate the adhesion work that portrays the overall cell-surface interaction throughout the whole unbinding process [54]. Therefore, when many minor molecular surface interactions are present between the cell probe and substrate, the energy of adhesion is the most reliable parameter to understand the overall adhesion process. Overall, adhesion force and adhesion energy measurements can both be found in the AFM literature, with some reports providing both maximum adhesion force and energy simultaneously [24]. Also, values for rupture lengths and contour lengths that represent the distance in which the cell or receptor detaches from the surface can also be found [15,18,19,28]. Overall, longer interaction distances are indicative of a stronger adhesive interaction between bacteria and surface or of the stretching of cellular components (such as the cell membrane or adhesins) as well as of the mechanical properties of the surface [51]. Finally, when molecular interactions are present (mostly in the form of "sawtooth" patterns in the force-distance curves) it is also possible to quantify the specific adhesion force of the adhesins involved in binding of the substrate [14]. Taken altogether, this array of adhesion parameters can paint a picture of the dynamics of bacterial adhesion to surfaces at both the cellular and sub-cellular levels.

On the other hand, there are several experimental settings that can impact the data resulting from AFM-based adhesion experiments. Ideally, all adhesion experiments involving bacteria should be carried out in buffer conditions instead of air to maintain bacterial viability and be biologically comparable with the in-vivo bacteria-substrate interaction [52]. Furthermore, it is crucial to ideally select soft AFM cantilevers with reduced spring constants (~0.01–0.1 N/m) to be able to detect adhesion forces in the cellular and sub-cellular range (nN to pN) [19,52,55]. The choice of force-spectroscopy over dynamic modes is also usually preferred to quantify bacterial adhesion parameters and maintain a precise control of the applied force during the experiment. As observed in the analyzed studies, bacteria can experimentally be either immobilized to the AFM tip or the substrate to probe their adhesive behavior, which will depend on factors such as the particular biological question being assessed, the cellular morphology of the microorganisms, and technical capacities (Fig. 1, Table 1). Overall, these parameters are crucial to ensure the reproducibility and biological significance of AFM findings regarding oral bacterial adhesion to biomaterials.

As with other in-vitro studies, there are some limitations that must be considered when discussing the primary papers included in this review. Firstly, AFM experiments are in-vitro experiments that although carried out in near-physiological conditions, may not be indicative of how bacteria effectively attach in some in-vivo situations. The oral cavity is a highly complex and multivariable niche, and it remains difficult to completely translate it into a laboratory setting [56,57]. Furthermore, as AFM is such a sensitive technique, the presence of multiple variables in the experimental setup (such as patient-derived specimens or saliva) can difficult standardization of results and reproducibility. Thus, the study of the adhesion of oral bacteria to relevant surfaces is frequently explored in a 'simplified' approach compared to the true oral setting, such as by the use of physiological buffers at a stable physiological temperature [58]. Nevertheless, AFM bacterial spectroscopy can yield quantifiable data regarding oral bacterial adhesion at the cellular and molecular level that is not possible to obtain with most other microscopy techniques and microbiological assays. Taken altogether, living cell bacterial adhesion experiments with AFM can explore the dynamics of oral bacteria colonization of surfaces and generate new knowledge on how to develop new approaches against biofilm formation in the context of oral biofilm-mediated diseases. This knowledge should be considered for the design of new molecules and oral biomaterials to selectively reduce bacterial adhesion and thus decrease the probability of developing biofilm-mediated diseases in the oral cavity.

5. Conclusions

This review highlights the current use of AFM to study the real-time adhesion of living oral bacteria onto tissues and biomaterials of clinical interest. The included studies demonstrate that bacterial attachment is modulated by cell-surface contact time, surface roughness and antifouling properties, bacteria strain type, glycation, and the presence or absence of fluor. Current antibacterial approaches should consider these variables when designing molecules and surfaces to counteract oral biofilm formation and prevent the development of disease in the oral cavity.

Declaration of Competing Interest

There are no conflicts of interest to declare for this work.

Acknowledgements

This work was supported by the ANID FONDECYT #1220804 and ANID FONDEQUIP EQY230010 grants.

Appendix A. Supporting information

Supplementary data associated with this article can be found in the online version at doi:10.1016/j.jdsr.2025.03.002.

References

[1] Jin LJ, et al. Global burden of oral diseases: emerging concepts, management and interplay with systemic health. Oral Dis 2016;22:609–19.
[2] Wen PYF, Chen MX, Zhong YJ, Dong QQ, Wong HM. Global burden and inequality of dental caries, 1990 to 2019. 00220345211056247 J Dent Res 2021. https://doi.org/10.1177/00220345211056247.
[3] Hall-Stoodley L, Costerton J, Stoodley P. Bacterial biofilms: from the natural environment to infectious diseases. Nat Rev Microbiol 2004;2:95–108.
[4] Lamont RJ, Koo H, Hajishengallis G. The oral microbiota: dynamic communities and host interactions. Nat Rev Microbiol 2018;16:745–59.
[5] Hojo K, Nagaoka S, Ohshima T, Maeda N. Bacterial interactions in dental biofilm development. J Dent Res 2009;88:982–90.
[6] Parreira P, Martins MCL. The biophysics of bacterial infections: adhesion events in the light of force spectroscopy. Cell Surf 2021;7:100048.
[7] Berne C, Ellison CK, Ducret A, Brun YV. Bacterial adhesion at the single-cell level. Nat Rev Microbiol 2018;16:616–27.
[8] Yuan Y, Hays MP, Hardwidge PR, Kim J. Surface characteristics influencing bacterial adhesion to polymeric substrates. RSC Adv 2017;7:14254–61.
[9] Dufrêne YF. Atomic force microscopy, a powerful tool in microbiology. J Bacteriol 2002;184:5205–13.
[10] Mularski A, Wilksch JJ, Hanssen E, Strugnell RA, Separovic F. Atomic force microscopy of bacteria reveals the mechanobiology of pore forming peptide action. Biochim Biophys Acta Biomembr 2016;1858:1091–8.
[11] Cho DH, Aguayo S, Cartagena-Rivera AX. Atomic force microscopy-mediated mechanobiological profiling of complex human tissues. Biomaterials 2023;303:122389.
[12] Aguayo S, Donos N, Spratt D, Bozec L. Single-bacterium nanomechanics in biomedicine: unravelling the dynamics of bacterial cells. Nanotechnology 2015;26:062001.
[13] El-Kirat-Chatel S., Beaussart A.Probing bacterial adhesion at the single-molecule and single-cell levels by AFM-based force spectroscopy. in nanoscale imaging: methods and protocols (ed. Lyubchenko, Y.L.) 403–414 (Springer New York, New York, NY, 2018). doi:10.1007/978-1-4939-8591-3_24.2018.
[14] Beaussart A, El-Kirat-Chatel S. Microbial adhesion and ultrastructure from the single-molecule to the single-cell levels by atomic force microscopy. Cell Surf 2019;5:100031.
[15] Sharma S, et al. Nanoscale characterization of effect of L-arginine on Streptococcus mutans biofilm adhesion by atomic force microscopy. Microbiology 2014;160:1466–73.
[16] Wang C, Hou J, van der Mei HC, Busscher HJ, Ren Y. Emergent properties in Streptococcus mutans biofilms are controlled through adhesion force sensing by initial colonizers. mBio 2019;10.
[17] Vadillo-Rodríguez V, Busscher HJ, Norde W, De Vries J, Van Der Mei HC. Atomic force microscopic corroboration of bond aging for adhesion of Streptococcus thermophilus to solid substrata. J Colloid Interface Sci 2004;278:251–4.
[18] Das T, Sharma PK, Krom BP, Van Der Mei HC, Busscher HJ. Role of eDNA on the adhesion forces between streptococcus mutans and substratum surfaces: influence of ionic strength and substratum hydrophobicity. Langmuir 2011;27:10113–8.
[19] Leiva-Sabadini C, et al. Nanoscale dynamics of streptococcal adhesion to AGE-modified collagen. J Dent Res 2023;102:957–64.
[20] Schuh CMAP, et al. Modulatory effect of glycated collagen on oral streptococcal nanoadhesion. J Dent Res 2021;100:82–9.
[21] Doll-Nikutta K, et al. Adhesion forces of oral bacteria to titanium and the correlation with biophysical cellular characteristics. Bioengineering 2022;9.
[22] Busscher HJ, Van De Belt-Gritter B, Dijkstra RJB, Norde W, Van Der Mei HC. Streptococcus mutans and Streptococcus intermedius adhesion to fibronectin films are oppositely influenced by ionic strength. Langmuir 2008;24:10968–70.
[23] González-Benito J, Teno J, González-Gaitano G, Xu S, Chiang MY. PVDF/TiO2 nanocomposites prepared by solution blow spinning: surface properties and their relation with S. mutans adhesion. Polym Test 2017;58:21–30.
[24] Postollec F, Norde W, de Vries J, Busscher HJ, van der Mei HC. Interactive forces between co-aggregating and non-co-aggregating oral bacterial pairs. J Dent Res 2006;85:231–4.
[25] Dhall A, et al. Bimodal nanocomposite platform with antibiofilm and self-powering functionalities for biomedical applications. ACS Appl Mater Interfaces 2021;13:40379–91.
[26] Yu P, et al. Influence of surface properties on adhesion forces and attachment of streptococcus mutans to zirconia in vitro. Biomed Res Int 2016;2016.
[27] Wang R, Wang Y, Lei Z, Hao L, Jiang L. Glucosyltransferase-modulated Streptococcus mutans adhesion to different surfaces involved in biofilm formation by atomic force microscopy. Microbiol Immunol 2022;66:493–500.
[28] Zhu L, et al. Functional characterization of cell-wall-associated protein WapA in Streptococcus mutans. Microbiology 2006;152:2395–404.
[29] Busscher HJ, et al. Intermolecular forces and enthalpies in the adhesion of Streptococcus mutans and an antigen I/II-deficient mutant to laminin films. J Bacteriol 2007;189:2988–95.
[30] Loskill P, et al. Reduced adhesion of oral bacteria on hydroxyapatite by fluoride treatment. Langmuir 2013;29:5528–33.
[31] Mei L, Ren Y, Busscher HJ, Chen Y, van der Mei HC. Poisson analysis of streptococcal bond-strengthening on saliva-coated enamel. J Dent Res 2009;88:841–5.
[32] Boks NP, Busscher HJ, van der Mei HC, Norde W. Bond-strengthening in staphylococcal adhesion to hydrophilic and hydrophobic surfaces using atomic force microscopy. Langmuir 2008;24:12990–4.
[33] Tu Y, Ren H, He Y, Ying J, Chen Y. Interaction between microorganisms and dental material surfaces: general concepts and research progress. J Oral Microbiol 2023;15:2196897.
[34] Schüler V, Lussi A, Kage A, Seemann R. Glycan-binding specificities of Streptococcus mutans and Streptococcus sobrinus lectin-like adhesins. Clin Oral Investig 2012;16:789–96.
[35] Huang W, et al. Mechanical stabilization of a bacterial adhesion complex. J Am Chem Soc 2022;144:16808–18.
[36] Álvarez S, Leiva-Sabadini C, Schuh CMAP, Aguayo S. Bacterial adhesion to collagens: implications for biofilm formation and disease progression in the oral cavity. Crit Rev Microbiol 2021:1–13. https://doi.org/10.1080/1040841X.2021.1944054.
[37] Wang H, et al. Influence of fimbriae on bacterial adhesion and viscoelasticity and correlations of the two properties with biofilm formation. Langmuir 2017;33:100–6.
[38] Cross SE, et al. Nanomechanical properties of glucans and associated cell-surface adhesion of Streptococcus mutans probed by atomic force microscopy under in situ conditions. Microbiology 2007;153:3124–32.
[39] Aguayo S, Donos N, Spratt D, Bozec L. Probing the nanoadhesion of Streptococcus sanguinis to titanium implant surfaces by atomic force microscopy. Int J Nanomed 2016;11:1443–50.
[40] Siddiqui DA, Fidai AB, Natarajan SG, Rodrigues DC. Succession of oral bacterial colonizers on dental implant materials: an in vitro biofilm model. Dent Mater 2022;38:384–96.
[41] Doll K, et al. Liquid-infused structured titanium surfaces: antiadhesive mechanism to repel streptococcus oralis biofilms. ACS Appl Mater Interfaces 2019;11:23026–38.
[42] Preedy E, Perni S, Nipič D, Bohinc K, Prokopovich P. Surface roughness mediated adhesion forces between borosilicate glass and gram-positive bacteria. Langmuir 2014;30:9466–76.
[43] Ajdić D, et al. Genome sequence of Streptococcus mutans UA159, a cariogenic dental pathogen. Proc Natl Acad Sci USA 2002;99:14434–9.
[44] Shields RC, Zeng L, Culp DJ, Burne RA. Genomewide Identification of essential genes and fitness determinants of streptococcus mutans UA159. mSphere 2018;3.
[45] Lemos JA, et al. The biology of streptococcus mutans. Microbiol Spectr 2019;7. https://doi.org/10.1128/microbiolspec.gpp3-0051–2018.
[46] Ito S, et al. Specific strains of Streptococcus mutans, a pathogen of dental caries, in the tonsils, are associated with IgA nephropathy. Sci Rep 2019;9:20130.
[47] Kojima A, et al. Infection of specific strains of Streptococcus mutans, oral bacteria, confers a risk of ulcerative colitis. Sci Rep 2012;2:332.
[48] Nomura R, et al. Isolation and characterization of Streptococcus mutans in heart valve and dental plaque specimens from a patient with infective endocarditis. J Med Microbiol 2006;55:1135–40.
[49] Xu W, Zhou W, Wang H, Liang S. Roles of porphyromonas gingivalis and its virulence factors in periodontitis. Adv Protein Chem Struct Biol 2020;120:45–84.
[50] Dini C, et al. Progression of bio-tribocorrosion in implant dentistry. Front Mech Eng 2020;6.
[51] Aguayo S, Bozec L. Mechanics of bacterial cells and initial surface colonisation. In: Leake MC, editor. Biophysics of Infection. Cham: Springer International Publishing; 2016. p. 245–60. https://doi.org/10.1007/978-3-319-32189-9_15.
[52] Beaussart A, El-Kirat-Chatel S. Quantifying the forces guiding microbial cell adhesion using single-cell force spectroscopy. Nat Protoc 2014;9:1049–55.
[53] Viljoen A, Mignolet J, Viela F, Mathelié-Guinlet M, Dufrêne YF. How microbes use force to control adhesion. J Bacteriol 2020;202.
[54] Hofschröer V, et al. Extracellular protonation modulates cell-cell interaction mechanics and tissue invasion in human melanoma cells. Sci Rep 2017;7:42369.
[55] Marshall H, et al. In vivo relationship between the nano-biomechanical properties of streptococcal polysaccharide capsules and virulence phenotype. ACS Nano 2020;14.
[56] Luo TL, et al. In vitro model systems for exploring oral biofilms: from single-species populations to complex multi-species communities. J Appl Microbiol 2022;132:855–71.
[57] Xu X, et al. Oral cavity contains distinct niches with dynamic microbial communities. Environ Microbiol 2015;17:699–710.
[58] Dufrêne YF, Viljoen A, Mignolet J, Mathelié-Guinlet M. AFM in cellular and molecular microbiology. Cell Microbiol 2021;23:e13324.